First-Principles Study of Water Chains Encapsulated in Single-Walled Carbon Nanotube

Lu Wang,[†] Jijun Zhao,*[,†] Fengyu Li,[†] Haiping Fang,[‡] and Jian Ping Lu[§]

School of Physics and Optoelectronic Technology and College of Advanced Science and Technology, Dalian University of Technology, Dalian 116024, China, Shanghai Institute of Applied Physics, Chinese Academy of Sciences, Shanghai 201800, China, and Department of Physics and Astronomy, University of North Carolina at Chapel Hill, Chapel Hill, North Carolina 27599

Received: October 7, 2008; Revised Manuscript Received: February 6, 2009

Water molecules confined inside a single-walled (6, 6) carbon nanotube were investigated using density functional theory. In this narrow-sized carbon nanotube (of about 0.8 nm in diameter), the encapsulated water molecules form chain-like configurations via hydrogen bonding. As compared to the water chains in vacuum, the intramolecular charge transfer in the encapsulated water chain is enhanced and the dipole moment is reduced due to the screening effect of the carbon nanotube. The tube−molecule interaction characterized by the coupling energy is about 0.28 eV per water molecule by local density approximation and 0.1 eV by general gradient approximation; the latter one is close to the results by empirical potentials. Weak coupling between the molecular orbitals of the encapsulated water molecules and the delocalized π electrons from the carbon nanotube was observed, implying that the tube−water interaction is not a simple effect of geometry confinement. Vibrational analysis revealed some unique hydrogen-bond modes for the water chains as well as red shift of the O−H stretching modes for the encapsulated water molecules with regard to the vacuum frequencies due to the tube−water interaction.

1. Introduction

Water in nanoscale environments is of great importance for biological activity of macromolecules as well as for designing novel molecular devices. In recent years, there have been raising interests in the encapsulation of water inside the nanoscale channels such as carbon nanotubes (CNTs), because the nanotube can provide a confining geometry without a strong interaction but still influence the hydrogen bonding. So far, the behavior of the water molecules encapsulated inside nanoscale channels (in particular, carbon nanotubes) has been extensively studied.[1−43]

In recent experiments, water molecules have been successfully filled into carbon nanotubes, and the morphologies of the confined water systems have been obtained.[1−6] For instance, Gogotsi et al. observed the incorporation of water into CNTs[1] and found strong atomic-scale interactions between the entrapped liquid-phase water and the graphite layers. Naguib et al.[2] presented a method to fill the multiwalled carbon nanotubes of 2−5 nm in diameter with an aqueous fluid and performed in situ high-resolution observations of the fluid behavior in this confined system. Kolesnikov's neutron scattering experiments[3] clearly showed the entry of water into the open-ended single-walled nanotube and identified an ice-shelled structure by water chains. More recently, Holt and co-workers revealed that the water flow rate through a CNT is 3 orders of magnitude faster than the conventional nonslip hydrodynamic flow.[4]

Studying the water inside nanoscale confined environments such as carbon nanotubes has attracted great interest mainly due to the following two reasons. First, as a result of nanoscale confinement, the chemical and physical properties of the encapsulated water are expected to differ from the bulk counterparts. A variety of new phases was observed due to the influences of water−wall interaction, small channel diameter, and hydrogen-bonding interaction between water molecules.[7−16] For example, water confined inside a single-walled carbon nanotube (SWCNT) under axial pressure can exhibit either a first-order freezing transition into hexagonal and heptagonal ice nanotubes or a continuous phase transition into solid-like square or pentagonal nanotubes.[7] Mashl et al.[8] demonstrated that water inside a nanotube can display anomalous ice-like behavior in both symmetry and mobility while retaining a liquid-like degree of water−water hydrogen bonding. A similar liquid-to-gas transition inside some confined biological channels was also observed via numerical simulations.[16]

Second, the spatial dimensions of the carbon nanotubes are comparable to those of the ion channel in the naturally biological systems, providing a simple model environment to exploit the primary behavior of water in complex real biological systems. Understanding the water−tube interaction and the transport behavior of water molecules inside nanotube may shed some light on the relevant biological systems and lead to novel nanoscale devices for proton storage and transport applications. In particular, studying the water confined in nanoscale environments provides a better understanding of the proton transport across the channels in the cellular membrane that transport water in and out of the cell (aquaporins).[20−22] Recent molecular dynamics (MD) simulations have achieved great success in this aspect.[8,9,23−38] For example, flipping and gating of water permeation across the narrow nanoscale channels have been investigated by Fang's group.[25−28] With addition of external force (wall deformation)[25] or a charge close to the tube wall,[26] single-walled carbon nanotubes exhibit excellent on−off gating behavior in water transport. Fang et al. further proposed the design of a molecular water pump using a CNT nanopore.[27] Recently, Joseph and Aluru found enhanced flow rate arose from a velocity "jump" in the depletion region at the water/nanotube

* Corresponding author. E-mail: zhaojj@dlut.edu.cn.
[†] Dalian University of Technology.
[‡] Chinese Academy of Sciences.
[§] University of North Carolina at Chapel Hill.

10.1021/jp808873r CCC: $40.75
Published on Web 03/17/2009

TABLE 1: Computed Geometry Parameters and Physical Properties for Water Monomer and Dimer As Compared to Available Experimental Data[50−53]

monomer	O−H bond (Å)	H−O−H angle (deg)	dipole moment (debye)	ionization potential (eV)	frequency (cm^{-1})		
LDA	0.971	104.7	2.04	13.05	1575	3739	3860
PW91	0.969	103.7	1.99	12.81	1618	3724	3840
expt.	0.96[52]	103.9[52]	1.86[51]	12.65[52]	1595[52]	3657	3756

					frequency (cm^{-1})	
dimer	O−O distance (Å)	strength of hydrogen bond (kcal/mol)	dipole moment (debye)	ionization potential (eV)	free O−H stretching	hydrogen-bonded O···H
LDA	2.75	9.56	2.83	10.84	3715	3466
PW91	2.887	5.64	2.82	10.74	3723	3576
expt.	2.98[53]	5.0 ± 0.7[53]	2.64[53]	11.21[52]	3730[50]	3601

interface.[30] Sood's group studied the structure and dynamics of single-file water inside the carbon nanotube via MD simulations[35] and proposed a one-dimensional (1D) random walk model for the diffusion behavior.

Vibrational spectroscopy is an important mean to characterize the structure and hydrogen-bonding behavior of the confined water molecules. Martí and Gordillo performed MD simulations for the liquid water confined in carbon nanotube, and they observed a new high-frequency mode around 3650 cm^{-1}.[17] Feng et al. simulated the infrared and resonant Raman spectra of ice nanotubes encapsulated inside a carbon nanotube using density functional tight-binding method.[18] They found that hydrogen bond plays an important role not only in the formation of the unique structures of ice nanotube but also in the signatures of vibrational spectra. Adsorption and desorption of water molecule on SWCNTs was experimentally investigated by Sharma et al. using Raman spectroscopy.[19] Recently, Byl et al.[11] presented an experimental vibrational spectroscopy study of water confined inside CNT, and they reported a distinct sharp vibrational mode associated with a distorted hydrogen bond of the confined water at 3507 cm^{-1}. This phenomenon has been interpreted via theoretical simulations of water molecules confined in nanotube with different diameters using both first-principles methods and empirical MD approach.[10]

Despite the great successes in those previous theoretical studies for the tube/water hybrid systems, most of them were done with empirical MD simulations. The tube−water interaction was assumed to be of van der Waals (vdW) type modeled by the empirical potentials.[23−28] There have been only a few first-principles studies on the electronic properties, vibrational frequencies, behavior of hydrogen bonds, and one-dimensional proton transfer for the water molecules inside carbon nanotube.[10,18,29,39−42] However, the details of tube−water interaction and the behavior of the encapsulated water chain are still largely unclear. For example, how do the delocalized π electrons of CNT couple with the valence electrons of water molecule? What is the influence of the host−guest interactions on the strength of intermolecular hydrogen bonds and the physical properties (such as dipole moments, electron transfer, and vibrational frequencies) of the water molecular clusters?

To address these issues, here we present DFT calculations of the 1D chains of $(H_2O)_n$ ($n = 1-5$) clusters encapsulated inside a finite-length (6, 6) SWCNT and discuss the electronic and vibrational properties of the hybrid systems. The main purpose of this study is to gain a deep insight into the behaviors of the encapsulated water chain and the tube−water interaction that are not accessible from pure empirical simulations. We observed weak coupling between the molecular orbitals of CNT and water molecules. Vibrational analysis revealed some unique hydrogen-bond participated vibrational modes for the 1D water chains as well as red shift of the O−H stretching modes of the encapsulated water molecules with regard to the vacuum values due to the tube−water interaction.

2. Computational Methods

Our model system consists of a finite-length (6, 6) SWCNT with two open ends terminated by hydrogen atoms, which has been frequently employed in MD simulation of the transport behavior of 1D water.[23−29] The (6, 6) SWCNT segment includes 144 carbon atoms and 24 hydrogen atoms with the diameter of 0.85 nm and the length of 1.5 nm. Initially, one to five water molecules with random orientations were arbitrarily placed inside the tube. Upon relaxation, these water molecules form ordered chain-like structures inside CNT, regardless of the initial configurations.

All computations are performed using all-electron DFT calculations with a double numerical basis set plus d-polarization functions (DNP), as implemented in the DMol^3 program.[44] Self-consistent field calculations were done with a convergence criterion of 10^{-6} a.u. on the total energy. All structures were optimized with convergence criteria of 10^{-6} a.u. on the maximum force and 0.005 Å on the maximum displacement of each atom. The real-space global orbital cutoff radius was chosen to be 5.0 Å.

It is well-known that standard density functional theory within either local density approximation (LDA) or generalized gradient approximation (GGA) cannot reproduce the weak vdW interactions accurately. Previous benchmark calculations on the noncovalent interactions between small molecules (such as benzene−ammonia complex,[45] methane dimer,[46] ethylene dimer, water−methanol complex, and others[47]) showed that LDA typically overestimates the intermolecular binding energy, while the PW91 parametrization within GGA is closer to high-level MP2 results but usually underestimates the binding. Here, both LDA[48] and GGA-PW91[49] were employed to describe the exchange-correlation interaction. It is expected that LDA and GGA results may roughly set the upper and lower bounds for the true coupling energy between water molecules and carbon nanotube.

To assess the performance of the computational scheme, in Table 1 we compare the computed geometry parameters and physical properties of water monomer and dimer with available experimental data.[50−54] Overall speaking, LDA cannot accurately describe the geometry (underestimation of the O−O distance of the water dimer by 8%), bonding and electronic properties (overestimation of the strength of hydrogen bond for water dimer by 95%), and vibrational properties (underestimation of the

frequency for the mode associated with hydrogen-bonded O···H by 135 cm^{-1}), while GGA-PW91 results agree reasonably with the experimental data.

We have also computed the interaction energy between a H_2O molecule and a $C_{54}H_{18}$ model of graphene sheet, which is 0.22 eV by LDA and 0.09 eV by GGA-PW91, respectively. As compared to a previous theoretical value of 0.11 eV at MP2/6-31G(d) level[55] and the experimental water−graphite interaction energy of 0.08 eV,[56] it seems that GGA-PW91 is relatively satisfactory for describing such weak molecule−surface interaction. Therefore, in this work, the majority of the theoretical results of water−tube interaction were obtained using the GGA-PW91 functional except that we included some LDA results for comparison.

To characterize the inter-water molecular interaction and the interaction between the water molecules and CNT, we define the binding energy per water molecule (E_B) and the coupling energy per water molecule (E_C), respectively. E_B measures the average interaction between a water molecule and its environment, including the intermolecular interaction within the water chains and the interaction between this water molecule and the nanotube. E_B can be calculated using the following formula:

$$E_B = -(E_{complex} - E_{tube} - nE_{water})/n \quad (1)$$

$E_{complex}$ is the total energy of the water/tube hybrid complex; E_{tube} is the total energy of the finite-length (6, 6) SWCNT; E_{water} is the total energy of an individual water molecule; and n is the number of water molecules.

To separate the inter-water molecular interaction and the tube−water coupling interaction, here we define the coupling energy per water molecule (E_C) as:

$$E_C = -(E_{complex} - E_{tube} - E_{chain})/n \quad (2)$$

where E_{chain} is the total energy of the water chain in vacuum, which has the same configuration as was encapsulated in the CNT.

3. Results and Discussion

3.1. Structures and Energetics. Upon relaxation, the randomly placed water molecules inside CTN tend to form ordered configuration, a water chain, due to the geometry confinement of the nanotube wall as well as the intermolecular hydrogen bonds. Each water molecule is hydrogen-bonded with one or two neighboring water molecules, forming a zigzag chain. Obviously, the number of hydrogen bonds per molecule in the encapsulated water chain is fewer than the number (three to four) in the condensed phases such as the liquid water and the crystalline ice. Similar chain configurations have been observed in the snapshots of water molecules transport through nanotube in previous MD simulations.[9,10,24] Meanwhile, chain-like configurations of water molecules also exist in the other systems, for example, naturally biological systems such as the purple bacteria Rhodobacter Spaeroides,[57] the protein channels,[58] and the supercritical water and steam at high temperatures and low densities.[59−62]

Equilibrium geometries of water chains with one to five water molecules confined inside a finite (6, 6) SWCNT are shown in Figure 1. We found that the equilibrium configurations are insensitive to the choice of DFT functionals. Thus, only configurations by GGA-PW91 calculations are described below in detail as representative.

When one water molecule is encapsulated inside the nanotube, hydrogen atoms in the water molecule do not align parallel to the direction of tube axis, but orientate to the carbon nanotube wall (perpendicular to the tube axis). This perpendicular orientation is energetically preferred by 0.013 eV over the parallel orientation. As compared to the gas-phase molecule, the changes in the bond angle and the bond length for the molecular geometry are rather small, that is, less than 1%. Similar orientation of the water molecule also occurs in other cases, such as liquid water near the flat hydrophobic surface,[63] water confined inside the graphite channels[64] or graphite surface,[65] and water at the vapor/water interface.[66]

When two water molecules were randomly placed inside the tube, upon relaxation the two molecules form a hydrogen-bonded dimer with the same configuration as that in the gas phase.[54,67−69] The theoretical O−O distance of the encapsulated water dimer is 2.884 Å, less than that of gas-phase water dimer (2.894 Å) at the same level of theory.

Three to five water molecules encapsulated inside the nanotube are aligned to a 1D water chain. To further discuss the geometry details of the water chains, we defined three characteristic angles α, β, and γ between hydrogen bonds (see Figure 1). The angle α in the confined $(H_2O)_3$ chain is 127.3°, and the average O−O distance is 2.793 Å. For the confined $(H_2O)_4$ chain, the values of α and β angles are 141.1° and 133.3°, respectively, with the average O−O distance of 2.77 Å. The angles of α, β, and γ for the $(H_2O)_5$ chain inside the CNT are 123.4°, 102.1°, and 105.9°, respectively, with the average O−O distance of 2.751 Å. Note that the chain configurations for the $(H_2O)_3$, $(H_2O)_4$, and $(H_2O)_5$ molecular clusters only exist stably in the 1D confined environments. In the gas phase, they will transform into cyclic structures upon relaxation.[54,67−69] For those encapsulated water chains, the average lengths for the non-hydrogen-bonded and hydrogen-bonded O−H covalent bonds are 0.971 and 0.990 Å, respectively, comparable to the O−H bond lengths of 0.973 and 1.005 Å from a previous first-principles molecular dynamics simulation.[29] As the number of water molecules increases, the average O−O distance between neighboring water molecules is gradually shortened, that is, from 2.884 Å for $(H_2O)_2$ to 2.751 Å for $(H_2O)_5$. In a previous first-principles calculation,[39] the O−O distance for a long water chain inside CNT was found to be 2.6 Å.

Table 2 summarizes the binding energy E_B and coupling energy E_C per water molecule from LDA and GGA calculations. E_B and E_C as functions of n (number of water molecules) are displayed in Figure 2. The binding energy E_B describes the interaction between each water molecule and its overall environment. In both cases of LDA and GGA, E_B ascends as the number of water molecule inside the chain increases, gradually approaching its asymptotic limit for an infinite molecular chain (about 0.753 eV for LDA and 0.394 eV for GGA by extrapolation to large n).

Subtracting the intermolecular interaction of a gas-phase water chain from the E_B of confined water chain yields the coupling energy E_C, which measures the tube−water interaction of the hybrid system. As shown in Table 2 and Figure 2, the computed E_C is rather insensitive to the number of water molecules. The definition of E_C value is divided by the number of water molecules; thus it reflects the interaction between each water molecule and the outer nanotube, which is nearly independent of the other water molecules. This is a characteristic of such weakly noncovalent interaction. On average, the coupling energy per molecule is about 0.28 eV by LDA and 0.1 eV by GGA-

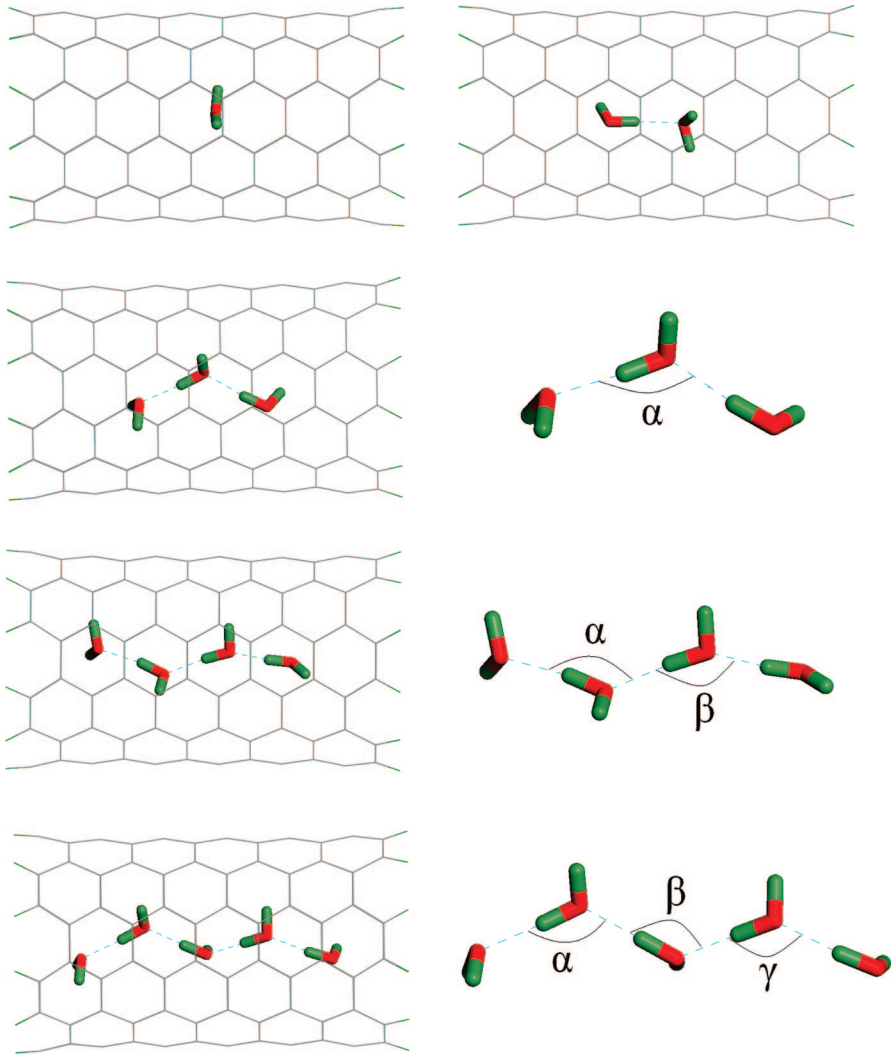

Figure 1. Equilibrium geometries of water chains confined in a (6, 6) carbon nanotube with definition of different characteristic angles. The green cylinder and red cylinder indicate hydrogen atom and oxygen atom, respectively.

TABLE 2: Binding Energy (E_B) and Coupling Energy (E_C) per Water Molecule Calculated by LDA, GGA-PW91, and Empirical Potentials

	E_B (eV)			E_C (eV)		
system	LDA	PW91	TIP3P+LJ	LDA	PW91	TIP3P+LJ
H_2O	0.271	0.120	0.073	0.271	0.120	0.073
$(H_2O)_2$	0.479	0.240	0.237	0.276	0.108	0.103
$(H_2O)_3$	0.580	0.300	0.289	0.281	0.104	0.083
$(H_2O)_4$	0.644	0.324	0.306	0.284	0.103	0.076
$(H_2O)_5$	0.665	0.347	0.346	0.276	0.100	0.106

PW91, respectively. Because LDA typically overestimates the weak interaction while GGA might underestimate, we expect that the true tube−water coupling energy lies between the LDA and GGA values, that is, within 0.1−0.28 eV.

In previous MD simulations, empirical intermolecular force fields such as TIP3P plus Lennard-Jones potential were frequently used to describe the water/tube hybrid systems. For comparison, here we calculated the E_B and E_C for the water chains with one to five molecules encapsulated inside the finite (6, 6) carbon nanotube (the configurations in Figure 1) using the same set of empirical parameters in the previous studies,[9,10,25−28] that is, TIP3P potential[70] for water−water interaction and Lennard-Jones potential with parameter ε_{CO} = 4.94 meV and σ_{CO} = 3.28 Å for water−tube interaction. The results from empirical potentials are also included in Figure 2 and Table 1. For both binding energy and coupling energy, it is interesting to find that the empirical TIP3P/LJ results are rather close to the GGA-PW91 ones, but significantly lower than those from LDA calculations.

3.2. Electronic Properties. To further explore the interaction between the water molecules and the outer nanotube, some characteristic electronic properties such as on-site charge transfer, molecular orbitals, and dipole moments were computed for the water/tube hybrid systems. The theoretical results are summarized in Table 3.

Mulliken population analysis shows that CNT environment influences the intramolecular electron transfer within each water molecule. As compared to the water molecular chain in a vacuum with the same configuration, the average electron transfer from hydrogen atoms to oxygen atom per molecule is slightly enhanced in the encapsulated water chains. For the water monomer, two hydrogen atoms totally donate 0.51 electrons to oxygen atom in the gas phase and 0.54 electrons in the confined phase. Such enhanced intramolecular charge transfer was observed consistently for all cases with different number of water molecules. As shown in Table 3, the difference of average electron transfer between the confined phase and the gas phase is all about 0.03e per molecule for all systems studied. Careful examination of the on-site charge on carbon nanotube shows that there is nearly no charge transfer between the CNT and the encapsulated water molecules.

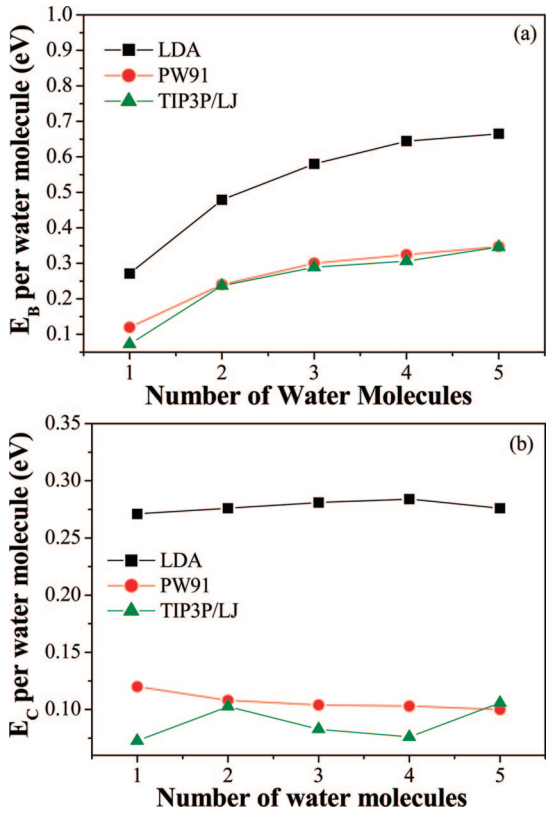

Figure 2. Plots of (a) binding energy E_B and (b) coupling energy E_C per water molecule as functions of number of water molecules from LDA, PW91, and empirical potentials calculations.

TABLE 3: Average Electron Transfer per Molecule from Hydrogen Atoms to Oxygen Atoms as the Water Molecule Increases from GGA-PW91 Calculations

system	inside SWCNT (e)	in a vacuum (e)
H_2O	0.54	0.51
$(H_2O)_2$	0.57	0.54
$(H_2O)_3$	0.59	0.56
$(H_2O)_4$	0.60	0.57
$(H_2O)_5$	0.6	0.57

We further discuss the tube−water interaction by analyzing the electron density of states (DOS) and the molecular orbitals near the highest occupied molecular orbital (HOMO). The DOS for the water/tube hybrid system is roughly a superposition of the DOS for the individual CNT and the gas-phase water molecules. There is no overlap of electron density in the empty region between the water molecule and CNT, indicating that the tube−molecule interaction has no covalent characteristic. The same conclusion was obtained in previous DFT[39−42] or DFTB[18] calculations of water molecules (in form of ice tube) encapsulated inside CNT.

However, the peak heights for several particular states on the DOS are moderately strengthened or weakened due to the water−tube interaction. Such a coupling interaction can be more clearly seen in the plots of the corresponding molecular orbitals. As representatives, the wave functions of the HOMO−3 and HOMO−4 states for the encapsulated $(H_2O)_5$ chain inside CNT are shown in Figure 3. These two delocalized states come from the π electrons of the carbon nanotube, while there is a small amount of π electrons distributed on the encapsulated water molecules. In other words, there is still weak coupling between the π electrons of the CNT and the valence electrons of the water molecules. Such weak tube−molecule coupling may affect

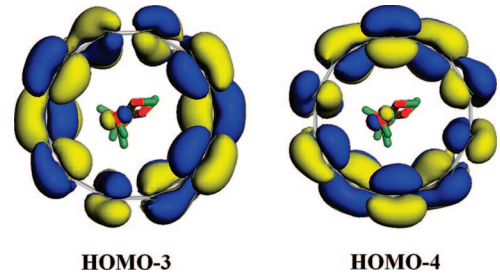

Figure 3. Isosurface for the wave functions of the HOMO−3 (left) and HOMO−4 (right) for $(H_2O)_5$ chain confined in a finite (6, 6) carbon nanotube. Yellow (blue) corresponds to positive (negative) values of the wave function.

TABLE 4: Dipole Moment Vectors (μ_x, μ_y, μ_z) and Dipole Moments ($|\mu|$) of the Water Chains Inside a (6, 6) Carbon Nanotube from GGA-PW91 Calculations

system	inside nanotube (μ_x, μ_y, μ_z), $\|\mu\|$ (debye)	in a vacuum (μ_x, μ_y, μ_z), $\|\mu\|$ (debye)
H_2O	(0.2, −0.38, −0.05), 0.44	(0.93, −1.74, −0.21), 1.98
$(H_2O)_2$	(0.02, 0.08, 0.53), 0.54	(0.2, 0.06, 2.76), 2.77
$(H_2O)_3$	(−0.18, 0.06, 0.80), 0.82	(−0.75, 0.12, 4.28), 4.34
$(H_2O)_4$	(0.38, 0.39, 1.48), 1.57	(1.44, 1.55, 7.25), 7.54
$(H_2O)_5$	(−0.62, 0.45, 2.13), 2.26	(−2.32, 1.7, 9.69), 10.11

the electronic and vibrational properties of the encapsulated water molecules, as we will discuss below.

It is known that many biological molecules carry a certain amount of dipole moments and the changes of dipole moments affect the intermolecular interaction, biomolecular salvation, as well as biochemical activities. Thus, it would be interesting to explore the effect of 1D nanoscale confinement on the dipole moment of the encapsulated water molecules. Listed in Table 4 are the electric dipole vectors and the amplitude of dipole moments of the water/tube complex, along with the values for the gas-phase water chains in vacuum. In both the gas phase and the confined phase, the dipole moments for the water chains with $n = 2-5$ are preferably aligned in the 1D chain direction, which is also the tube axis direction for the case of encapsulated water molecules. When the water chains are encapsulated inside the CNT, the dipole moments of the entire systems are drastically reduced by a factor of about 4.5−5.5 with respect to the vacuum values. This effect can be understood by the screening of the conducting electrons due to the outer carbon nanotube. When encapsulated inside CNT, the polarized water molecules would induce an inversed dipole moment on the nanotube, and the cancelation of induced moment on the nanotube and dipole moment on the water chains leads to a relatively smaller dipole moment with regard to moment of the gas-phase water molecules. Examination of the on-site Mulliken charge confirms this argument. A similar screening effect was observed in previous studies for water molecules confined in carbon nanotubes[29,41] and fullerenes.[71]

3.3. Vibrational Frequencies. Vibrational spectroscopy is one of the major experimental means to characterize the structural and bonding behavior of water systems,[72−76] and it is extremely sensitive to geometric structure and electronic properties. A detailed analysis of the vibrational frequencies in the water clusters enables one to understand the hydrogen bonding and to predict the structural pattern. Previously, there were numerous experimental and theoretical studies on the vibrational frequencies for crystalline ice,[77,78] liquid water,[79,80] and water clusters,[81−90] but few studies on those of water molecules encapsulated inside the carbon nanotube.[10,17−19,91] To make some theoretical predictions on both water−water hydrogen-bonding

TABLE 5: Vibrational Frequencies for Water Chains in the Gas Phase and in the Confined Phase with the Same Configuration

system	O−H stretching (asym.)	O−H stretching (sym.)	O−H stretching (H-bond assisted)	H−O−H bending
H_2O	3833	3720		1621
H_2O@CNT	3821	3712		1609
$(H_2O)_2$	3816, 3800	3706	3548	1648, 1623
$(H_2O)_2$@CNT	3796, 3785	3696	3531	1646, 1611
$(H_2O)_3$	3809, 3793, 3785	3699	3490, 3434	1672, 1649, 1620
$(H_2O)_3$@CNT	3794, 3786, 3768	3685	3472, 3410	1674, 1648, 1607
$(H_2O)_4$	3808, 3801, 3793, 3788	3699	3477, 3451, 3370	1672, 1663, 1645, 1619
$(H_2O)_4$@CNT	3788, 3786, 3776, 3757	3686	3455, 3435, 3348	1671, 1653, 1641, 1610
$(H_2O)_5$	3801, 3786, 3785, 3784, 3774	3693	3474, 3416, 3353 3275	1680, 1662, 1646, 1633, 1615
$(H_2O)_5$@CNT	3783, 3779, 3773, 3767, 3758	3680	3459, 3397, 3332, 3250	1681, 1663, 1644, 1631, 1600

interaction and water−tube interaction that can be assessed by future experiments, here we computed the vibration properties of the water chains encapsulated inside CNT using the standard frozen phonon method. For comparison, we considered the water chains in a vacuum with the same geometry configuration. The computational frequencies associated with the vibration of the water molecules are summarized in Table 5. The error bar of the present calculations should be within 2%, estimated from the comparison of the experimental and computational frequencies for the water monomer and dimer (see Table 1).

Vibrational spectroscopy of the O−H stretching mode is a sensitive indicator of the strength and coordination of the hydrogen bond. For both confined phase and gas phase, we found that the formation of water chain due to hydrogen bonding leads to significant modifications of the symmetric O−H stretching modes, while the effects on the other modes (i.e., asymmetric O−H stretching and H−O−H bending) are much less pronounced. Taking $(H_2O)_4$@CNT system as a representative, we plot the main vibrational directions for those O−H stretching modes in Figure 4. Generally speaking, for a water chain with n molecules, there is one asymmetric O−H stretching mode on each water molecule. Meanwhile, there is only one symmetric O−H stretching mode that is compatible to the case of individual molecule. This mode locates on the water molecule whose O−H bonds have not participated in the intermolecular hydrogen bonding ("free hydrogen atoms"). For the rest $n - 1$ modes, in addition to the symmetric O−H stretching on each water molecule (see Figure 4), the intermolecular hydrogen bonds clearly participated in the vibration, and the corresponding

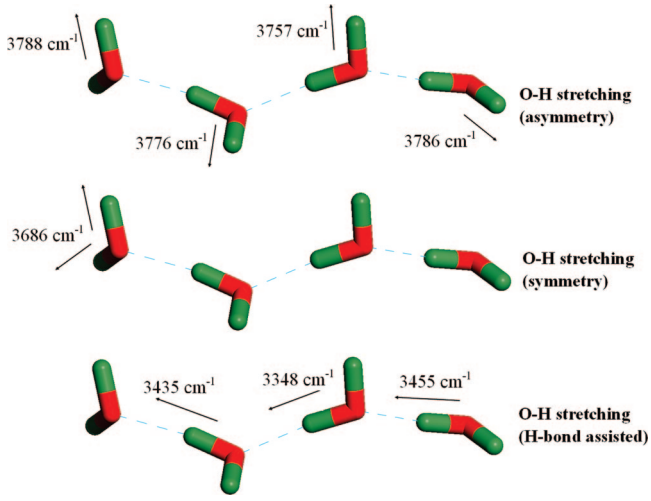

Figure 4. O−H stretching vibrational modes for $(H_2O)_4$ chain in the carbon nanotube. The green cylinder and red cylinder indicate the hydrogen atom and oxygen atom, respectively.

modes are denoted as the hydrogen-bond modes. The details on those hydrogen-bond modes will be discussed below.

As shown in Table 5, the computed frequencies for the hydrogen-bond modes associated with two-coordinated single donor are 3250−3550 cm^{-1}, while the frequency for the symmetric O−H stretching modes due to free hydrogen atoms is around 3700 cm^{-1}. This is consistent with a previous MD study of liquid water by Buch et al.,[80] who found that the vibrational modes with two-coordinated hydrogen bonds on the surface have frequencies in the range of 3250−3600 cm^{-1}, and the modes of free hydrogen atoms are around 3700 cm^{-1}. Similar vibrational modes associated with two-coordinated hydrogen bonds were also seen in the cyclic water clusters containing two to five molecules.[69,82] For comparison, three-coordinated molecules (double donor) within liquid water exhibit frequencies in the range of 3400−3700 cm^{-1},[80] whereas the vibration frequencies for three-coordinated and four-coordinated molecules in the water clusters are in the range of 3500−3700 and 3100−3700 cm^{-1}, respectively.[79] In other words, a larger number of hydrogen bonds would lead to wider frequency distribution for those O−H stretching modes. Finding of these characteristic O−H stretching modes in the 1D water clusters is useful to identify the chain configurations of water molecules in different environments such as in the carbon nanotube and the membrane of biological macromolecules.

For the water chains in both confined phase and gas phase (see Table 5), the frequencies for the H−O−H bending modes split and the several bending branches are somewhat related to the motion of water molecules. For the small-sized water chains like $(H_2O)_2$ and $(H_2O)_3$, different bending branches correspond to H−O−H bending vibration of individual water molecule. However, when the size of water chains increases, more than one water molecule would participate in one split bending branch, and all water molecules in the water chains contribute to each bending branch. The high-frequency end of the H−O−H bending modes is blue-shifted as the number of water molecules increases, for example, 1621 cm^{-1} for an individual water molecule and 1680 cm^{-1} for the $(H_2O)_5$ chain. Such blue shifts of H−O−H bending modes with increasing number of water molecules were also seen in previous studies on water clusters in the gas phase.[69,76,82]

In contrast, the O−H stretching modes are generally red-shifted with increasing number of molecules; for example, the symmetric O−H stretching mode is 3720 cm^{-1} for an individual water molecule and 3693 cm^{-1} for the $(H_2O)_5$ chain. Estimated from the present calculations, the average strength of each hydrogen bond increases from 0.263 eV for monomer to 0.308 eV for a pentamer chain in the gas phase. The enhanced strength of the intermolecular hydrogen bonds would weaken the strength

of intramolecular O−H bonds and result in red shifts of the O−H stretching modes.

Furthermore, comparison of the vibrational frequencies for the water chains in a vacuum and inside CNT may reflect the strength of the tube−water interaction. As shown in Table 5, encapsulation inside CNT leads to red shifts with an average magnitude of about 17 cm^{-1} for those O−H stretching modes of the water molecules. Similar red-shift phenomenon due to confinement was observed in previous studies.[11,17,18] For example, for a H_2O molecule inside (8, 8) nanotube, the red shift of the asymmetric and symmetric O−H stretching modes from Byl's calculations[11] is 16 and 5 cm^{-1}, respectively, while the frequency shifts are 12 and 8 cm^{-1} for H_2O@(6,6) tube from the present PW91/DNP calculations. For the O−H stretching vibration, the higher-frequency modes are more sensitive to the confinement than are the lower-frequency modes. This is consistent with Martí's results that the low-frequency band of liquid water confined inside nanotube does not show significant differences from bulk water.[17] For the H−O−H bending modes, the frequency changes due to water−molecule interaction are much less pronounced and not systematical, except for the H_2O@CNT in which the orientation of the water molecule is different (perpendicular to the CNT axis). The current theoretical predictions can be verified in future experiments on water molecules confined in various 1D environments.

4. Conclusion

First-principle calculations for the hybrid systems by water molecules confined inside a finite (6, 6) carbon nanotube were performed. The tube−water interactions were discussed in terms of the coupling energies, charge transfer, dipole moments, HOMO/LUMO distributions, and vibrational frequencies. Because of the geometry confinement by CNT as well as intermolecular hydrogen bonds, the encapsulated water molecules form 1D chain along tube axis. The coupling energy between CNT and water molecule is 0.28 eV per molecule by LDA and 0.1 eV by GGA-PW91; the latter is comparable to the results from the empirical Lennard-Jones potential (0.07−0.1 eV). The average electron transfer from hydrogen to oxygen is slightly enhanced inside the nanotube as compared to the water chain in vacuum with the same configuration. The dipole moments of the water/tube complex align in the direction along the tube axis, and they are significantly reduced from those of water chain in a vacuum due to the screening effect by CNT. Molecular orbital analysis shows weak coupling between valence electrons of water molecules and π electrons from the nanotube. Analysis of the vibrational modes for the water chains in both confined phase and gas phase reveals the characteristic O−H stretching modes associated with two-coordinated hydrogen bonds. With increasing number of water molecules, the frequencies of the H−O−H bending modes split and blue shift, while the O−H stretching modes red shift. The 1D confinement effect leads to red shifts of about 17 cm^{-1} for those O−H stretching modes, but has no systematical influence on the H−O−H bending modes.

The present results clearly indicate that even though the tube−water interaction is mainly vdW type, it is not simply a geometry confinement effect. There is still some weak coupling between the nanotube and the confined water chains, which modifies the electronic and vibrational properties of the water molecules to certain extents. In particular, we anticipate that the theoretical predictions on the vibrational frequencies of water molecular chain confined inside 1D confinement would motivate future experimental studies along this direction.

Acknowledgment. This work was supported by NCET-06-0281, the Natural Science Foundation of China (10774019, 40874039), and the Ph.D. Programs Foundation of the Education Ministry of China (20070141026).

References and Notes

(1) Gogotsi, Y.; Libera, J. A.; Yazicioglu, A. G.; Megaridis, C. M. *Appl. Phys. Lett.* **2001**, *79*, 1021.
(2) Naguib, N.; Ye, H.; Gogotsi, Y.; Yazicioglu, A. G.; Megaridis, C. M.; Yoshimura, M. *Nano Lett.* **2004**, *4*, 2237.
(3) Kolesnikov, A. I.; Zanotti, J. M.; Loong, C. K.; Thiyagarajan, P.; Moravsky, A. P.; Loutfy, R. O.; Burnham, C. J. *Phys. Rev. Lett.* **2004**, *93*, 035503.
(4) Holt, J. K.; Park, H. G.; Wang, Y.; Stadermann, M.; Artyukhin, A. B.; Grigoropoulos, C. P.; Noy, A.; Bakajin, O. *Science* **2006**, *312*, 1034.
(5) Majumder, M.; Chopra, N.; Andrews, R.; Hinds, B. J. *Nature* **2005**, *438*, 44.
(6) Zhao, Y.; Song, L.; Deng, K.; Liu, Z.; Zhang, Z.; Yang, Y.; Wang, C.; Yang, H.; Jin, A.; Luo, Q.; Gu, C.; Xie, S.; Sun, L. *Adv. Mater.* **2008**, *20*, 1772.
(7) Koga, K.; Gao, G. T.; Tanaka, H.; Zeng, X. C. *Nature* **2001**, *412*, 802.
(8) Mashl, R. J.; Joseph, S.; Aluru, N. R.; Jakobsson, E. *Nano Lett.* **2003**, *3*, 589.
(9) Hummer, G.; Rasaiah, J. C.; Noworyta, J. P. *Nature* **2001**, *414*, 188.
(10) Rasaiah, J. C.; Garde, S.; Hummer, G. *Annu. Rev. Phys. Chem.* **2008**, *59*, 713.
(11) Byl, O.; Liu, J. C.; Wang, Y.; Yim, W. L.; Johnson, J. K.; Yates, J. T., Jr. *J. Am. Chem. Soc.* **2006**, *128*, 12090.
(12) Waghe, A.; Rasaish, J. C.; Hummer, G. *J. Chem. Phys.* **2002**, *117*, 10789.
(13) Vaitheeswaran, S.; Rasaiah, J. C.; Hummer, G. *J. Chem. Phys.* **2004**, *121*, 7955.
(14) Maibaum, L.; Chandler, D. *J. Phys. Chem. B* **2003**, *107*, 1189.
(15) Zimmerli, U.; Gonnet, P. G.; Walther, J. H.; Koumoutsakos, P. *Nano Lett.* **2005**, *5*, 1017.
(16) Saparov, S. M.; Pohl, P. *Proc. Natl. Acad. Sci. U.S.A.* **2004**, *101*, 4805.
(17) Martí, J.; Gordillo, M. C. *Phys. Rev. B* **2001**, *63*, 165430.
(18) Feng, C.; Zhang, R. Q.; Dong, S. L.; Niehaus, Th. A.; Frauenheim, Th. *J. Phys. Chem. C* **2007**, *111*, 14131.
(19) Sharma, S. C.; Singh, D.; Li, Y. *J. Raman Spectrosc.* **2005**, *36*, 755.
(20) de Groot, B. L.; Grubmüller, H. *Science* **2001**, *294*, 2353.
(21) Tajkhorshid, E.; Nollert, P.; Jensen, M. O.; Miercke, L. J. W.; O'Connell, J.; Stroud, R. M.; Schulten, K. *Science* **2002**, *296*, 525.
(22) Murata, K.; Mitsuoka, K.; Hirai, T.; Walz, T.; Agre, P.; Heymann, J. B.; Engel, A.; Fujiyoshi, Y. *Nature* **2000**, *407*, 599.
(23) Waghe, A.; Rasaiaha, J. C.; Hummer, G. *J. Chem. Phys.* **2002**, *117*, 10789.
(24) Dellago, C.; Naor, M. M.; Hummer, G. *Phys. Rev. Lett.* **2003**, *90*, 105902.
(25) Wan, R. Z.; Li, J. Y.; Lu, H. J.; Fang, H. P. *J. Am. Chem. Soc.* **2005**, *127*, 7166.
(26) Li, J. Y.; Gong, X. J.; Lu, H. J.; Li, D.; Fang, H. P.; Zhou, R. H. *Proc. Natl. Acad. Sci. U.S.A.* **2007**, *104*, 3687.
(27) Gong, X. J.; Li, J. Y.; Lu, H. J.; Wan, R. Z.; Li, J. C.; Hu, J.; Fang, H. P. *Nat. Nanotechnol.* **2007**, *2*, 709.
(28) Fang, H. P.; Wan, R. Z.; Gong, X. J.; Lu, H. J.; Li, S. Y. *J. Phys. D: Appl. Phys.* **2008**, *41*, 103002.
(29) Mann, D. J.; Halls, M. D. *Phys. Rev. Lett.* **2003**, *90*, 195503.
(30) Joseph, S.; Aluru, N. R. *Nano Lett.* **2008**, *8*, 452.
(31) Longhurst, M. J.; Quirke, N. *Nano Lett.* **2007**, *7*, 3324.
(32) Whitby, M.; Quirk, N. *Nat. Nanotechnol.* **2007**, *2*, 87.
(33) Best, R. B.; Hummer, G. *Proc. Natl. Acad. Sci. U.S.A.* **2005**, *102*, 6732.
(34) Zhu, F. Q.; Schulten, K. *Biophys. J.* **2003**, *85*, 236.
(35) Mukherjee, B.; Maiti, P. K.; Dasgupta, C.; Sood, A. K. *J. Chem. Phys.* **2007**, *126*, 124704; *J. Nanosci. Nanotechnol.* **2007**, *7*, 1796.
(36) Li, H.; Zhang, X. Q.; Liew, K. M. *J. Chem. Phys.* **2008**, *128*, 034707.
(37) Maniwa, Y.; Matsuda, K.; Kyakuno, H.; Ogasawara, S.; Hibi, T.; Kadowaki, H.; Suzuki, S.; Achiba, Y.; Kataura, H. *Nat. Mater.* **2007**, *6*, 135.
(38) Takaiwa, D.; Hatano, I.; Koga, K.; Tanaka, H. *Proc. Natl. Acad. Sci. U.S.A.* **2008**, *105*, 39.
(39) Hanasaki, I.; Nakamura, A.; Yonebayashi, T.; Kawano, S. *J. Phys.: Condens. Matter* **2008**, *20*, 015213.
(40) Agrawal, B. K.; Singh, V.; Pathak, A.; Srivastava, R. *Phys. Rev. B* **2007**, *75*, 195421.

(41) Li, Y.; Lu, D.; Schulten, K.; Ravaioli, U.; Rotkin, S. V. *J. Comput. Electron.* **2005**, *4*, 161.
(42) Cicero, G.; Grossman, J. C.; Schwegler, E.; Gygi, F.; Galli, G. *J. Am. Chem. Soc.* **2008**, *130*, 1871.
(43) Alexiadis, A.; Kassinos, S. *Chem. Rev.* **2008**, *108*, 5014.
(44) Delley, B. *J. Chem. Phys.* **1990**, *92*, 508; *J. Chem. Phys.* **2000**, *113*, 7756.
(45) Enkvist, C.; Zhang, Y.; Yang, W. *Int. J. Comput. Chem.* **2000**, *79*, 325.
(46) Li, A. H.; Chao, S. D. *J. Chem. Phys.* **2006**, *125*, 094312.
(47) Tsuzuki, S.; Luthi, H. P. *J. Chem. Phys.* **2001**, *114*, 3949.
(48) Perdew, J. P.; Wang, Y. *Phys. Rev. B* **1992**, *45*, 13244.
(49) Perdew, J. P.; Chevary, J. A.; Vosko, S. H.; Jackson, K. A.; Pederson, M. R.; Singh, D. J.; Fiolhais, C. *Phys. Rev. B* **1992**, *46*, 6671.
(50) Huisken, F.; Kaloudis, M.; Kulcke, A. *J. Chem. Phys.* **1999**, *104*, 17.
(51) Lovas, F. J. *J. Phys. Chem. Ref. Data* **1978**, *7*, 1445.
(52) http://webbook.nist.gov/chemistry/ and references herein.
(53) Dyke, T. R.; Mack, K. M.; Muenter, J. S. *J. Chem. Phys.* **1977**, *66*, 498.
(54) Ludwing, R. *Angew. Chem., Int. Ed.* **2001**, *40*, 1808.
(55) Sudiarta, I. W.; Geldart, D. J. W. *J. Phys. Chem. A* **2006**, *110*, 10501.
(56) Helmy, A. K.; Ferreiro, E. A.; de Bussetti, S. G. *Appl. Surf. Sci.* **2007**, *253*, 4966.
(57) Stowell, M. H. B.; Mcphillips, T. M.; Rees, D. C.; Soltis, S. M.; Abresch, E.; Feher, G. *Science* **1997**, *276*, 812.
(58) Hille, B. *Ionic Channels of Excitable Membranes*; Sinauer: Sunderland, MA, 1984.
(59) Cummings, P. T.; Cochran, H. D.; Simonson, J. M.; Mesmer, R. E.; Karaborni, S. *J. Chem. Phys.* **1991**, *94*, 5606.
(60) Fois, E. S.; Sprik, M.; Parrinello, M. *Chem. Phys. Lett.* **1994**, *223*, 411.
(61) Ikushima, Y.; Hatakeda, K.; Saito, N.; Arai, M. *J. Chem. Phys.* **1998**, *108*, 5855.
(62) Buontempo, U.; Postorino, P.; Ricci, M. A.; Soper, A. K. *Mol. Phys.* **1994**, *81*, 217.
(63) Lee, C.-Y.; McCammon, J. A.; Rossky, P. J. *J. Chem. Phys.* **1984**, *80*, 4448.
(64) Martí, J.; Nagy, G.; Gordillo, M. C.; Guàrdia, E. *J. Chem. Phys.* **2006**, *124*, 094703.
(65) Pertsin, A.; Grunze, M. *J. Phys. Chem. B* **2004**, *108*, 1357.
(66) Du, Q.; Superfine, R.; Freysz, E.; Shen, Y. R. *Phys. Rev. Lett.* **1993**, *70*, 2313.
(67) Lee, C.; Chen, H.; Fitzgerald, G. *J. Chem. Phys.* **1995**, *102*, 1266.
(68) Xantheas, S. S.; Dunning, T. H., Jr. *J. Chem. Phys.* **1993**, *99*, 8774.
(69) Estrin, D. A.; Paglieri, L.; Corongiu, G.; Clementi, E. *J. Phys. Chem.* **1996**, *100*, 8701.
(70) Jorgensen, W. L.; Chandrasekhar, J.; Madura, J. D.; Impey, R. W.; Klein, M. L. *J. Chem. Phys.* **1983**, *79*, 926.
(71) Wang, L.; Zhao, J. J.; Fang, H. P. *J. Phys. Chem. C* **2008**, *112*, 11779.
(72) Vernon, M. F.; Krajnovich, D. J.; Kwok, H. S.; Lisy, J. M.; Shen, Y. R.; Lee, Y. T. *J. Chem. Phys.* **1982**, *77*, 47.
(73) Page, R. H.; Frey, J. G.; Shen, Y. R.; Lee, Y. T. *Chem. Phys. Lett.* **1984**, *106*, 373.
(74) Coker, D. F.; Miller, R. E.; Watts, R. O. *J. Chem. Phys.* **1985**, *82*, 3554.
(75) Huang, Z. S.; Miller, R. E. *J. Chem. Phys.* **1989**, *91*, 6613.
(76) Paul, J. B.; Provencal, R. A.; Chapo, C.; Roth, K.; Casaes, R.; Saykally, R. J. *J. Phys. Chem. A* **1999**, *103*, 2972.
(77) Devlin, J. P.; Buch, V. *J. Phys. Chem.* **1995**, *99*, 16534.
(78) Devlin, J. P.; Sadlej, J.; Buch, V. *J. Phys. Chem. A* **2001**, *105*, 974.
(79) Schmidt, D. A.; Miki, K. *J. Phys. Chem. A* **2007**, *111*, 10119.
(80) Buch, V. *J. Phys. Chem. B* **2005**, *109*, 17771.
(81) Ohno, K.; Okimura, M.; Akai, N.; Katsumoto, Y. *Phys. Chem. Chem. Phys.* **2005**, *7*, 3005.
(82) Dunn, M. E.; Evans, T. M.; Kirschner, K. N.; Shields, G. C. *J. Phys. Chem. A* **2006**, *110*, 303.
(83) Lenz, A.; Ojamäe, L. *J. Phys. Chem. A* **2006**, *110*, 13388.
(84) Anick, D. J. *J. Phys. Chem. A* **2006**, *110*, 5135.
(85) Schofield, D. P.; Kjaergaard, H. G. *Phys. Chem. Chem. Phys.* **2003**, *5*, 3100.
(86) Low, G. R.; Kjaergaard, H. G. *J. Chem. Phys.* **1999**, *110*, 9104.
(87) Miller, Y.; Fredj, E.; Harvey, J. N.; Gerber, R. B. *J. Phys. Chem. A* **2004**, *108*, 4405.
(88) Steinbach, C.; Andersson, P.; Kazimirski, J. K.; Buck, U.; Buch, V.; Beu, T. A. *J. Phys. Chem. A* **2004**, *108*, 6165.
(89) Sadlej, J.; Buch, V.; Kazimirski, J. K.; Buck, U. *J. Phys. Chem. A* **1999**, *103*, 4933.
(90) (a) Buck, U.; Ettischer, I.; Melzer, M.; Buch, V.; Sadlej, J. *Phys. Rev. Lett.* **1998**, *80*, 2578. (b) Buck, U.; Huisken, F. *Chem. Rev.* **2000**, *100*, 3863.
(91) Kondratyuk, P.; Yates, J. T., Jr. *Acc. Chem. Res.* **2007**, *40*, 995.

JP808873R